
Article:
Wu, X., Wang, M. and Lee, K.Y. (2020) Flexible operation of supercritical coal-fired power plant integrated with solvent-based CO2 capture through collaborative predictive control. Energy, 206. 118105. ISSN: 0360-5442

https://doi.org/10.1016/j.energy.2020.118105

Flexible Operation of Supercritical Coal-fired Power Plant Integrated with Solvent-based CO_2 Capture through Collaborative Predictive Control

Xiao Wu[a,*], Meihong Wang[b,*], Kwang Y. Lee[c]

[a]*Key laboratory of Energy Thermal Conversion and Control of Ministry of Education , Southeast Univerisity, Nanjing 210096, China*
[b]*Department of Chemical and Biological Engineering, Univerisity of Sheffield, Sheffield S1 3JD, UK*
[c]*Department of Electrical and Computer Engineering, Baylor University, One Bear Place #97356, Waco, TX 76798-7356, USA*

Abstract

This paper presents a controller design study for the supercritical coal fired power plant (CFPP) integrated with solvent-based post-combustion CO_2 capture (PCC) system. The focus of the study is on the steam drawn-off from turbine to the re-boiler, which is the key interaction between the CFPP and PCC plants. The simulation study of a 660MW supercritical CFPP-PCC unit model has shown that the impact of re-boiler steam change on the power generation of CFPP is more than 100 times faster than that on the PCC operation. Considering this finding, a collaborative predictive control strategy is proposed for the CFPP-PCC system where the re-boiler steam flowrate is manipulated for the CFPP load ramping and then gradually set to the required value for CO_2 capture. The PCC is thereby exploited as an energy storage device, which can quickly store/release extra energy for the CFPP in addition to the primary function of carbon emission reduction. The simulation results show that the proposed collaborative predictive controller can effectively improve the load ramping performance of CFPP without much performance degradation on the PCC operation.

Keywords: Supercritical coal-fired power plant; Solvent-based post-combustion carbon capture; Transient performance analysis; Flexible operation; Collaborative operation; Model predictve control.

1. Introduction

Fossil fuel-fired power stations (FFFPS) are still expected as pillars on which human society is built in a foreseeable future [1]. Implementing carbon capture technologies is thus important to reduce the carbon intensities of the FFFPS to meet the requirement of the 1.5 °C climate scenario by 2050 [2]. Solvent-based post-combustion CO_2 capture (PCC) has been regarded as the most promising near-term technology, which can reduce the CO_2 emission of FFFPS to less than 10% of its original level with minor retrofitting to the plant [3].

Besides developing PCC technologies to the FFFPS, replacing them with clean renewable energy sources such as wind and solar has been greatly promoted in the past decade [4]. However, the high penetration of renewable energies also leads to new regulatory questions owing to their intermittent features. According to the wind power integration statistics published by the National Energy Administration of China, the wind power curtailment in 2016 was 49.7 TWh, accounted for 17.1% of the total wind power generation [5]. This phenomenon can be exacerbated as the installed capacity of wind power continues to increase. In this context, the FFFPS has to shift its role from undertaking the baseload to quickly following the load change, so that the intermittent renewable power can be better integrated into the grid [6]. As a result, improving the load-following performance has become an urgent task for the FFFPSs to perform power balancing in the electricity grid; and consequently, flexible operation of the solvent-based PCC system has become one of the most important directions towards the large-scale commercialization in the power industry [7]. Mac Dowell and Shah [8] carried out a day-ahead scheduling study of PCC plant under given FFFPS flue gas and market conditions. They reported that the flexible operation of PCC can greatly enhance the economic performance of the integrated FFFPS-PCC system. Olaleye et al. [9] performed dynamic simulation on a supercritical coal-fired power plant (CFPP) model integrated with a PCC process. A further point made in their study was that flexible adjustment of the PCC re-boiler steam has the potential to improve the load ramping ability of the power plant.

Adaptation to the flue gas flowrate of upstream FFFPSs and altering the CO_2 capture level in accordance with the external

* Corresponding author.
E-mail address: wux@seu.edu.cn (X. Wu); Meihong.Wang@sheffield.ac.uk (M. Wang)

needs are two requests involved in the flexible operation of the solvent-based PCC process. Developing a rational control system for the PCC plant to attain a fast and smooth transition between different working conditions is thus the key issue to be solved [10].

A prerequisite for PCC control design is to understand the dynamic behavior of the system. Recent studies have developed detailed dynamic models for various process configurations using different approaches [11, 12] and carried out model validations based on the experimental data to demonstrate the model fidelities [13]. In-depth knowledge of the PCC plant has then been provided through the simulations, where the dynamic interactions among main process variables have been assessed [14]. Their results indicated that large response time in the scale of hours is expected for the PCC system when the re-boiler steam flow rate changes, whereas the change of lean solvent flowrate has relatively quick influence on the CO_2 capture level [15]. In view of this insight, many studies have suggested a general control structure for the solvent-based PCC process, where the sump levels are regulated by the liquid outlet valves; the pressures are regulated by the vapor outlet valves; temperatures of the re-boiler, condenser and lean solvent are regulated by the flowrates of steam/cooling water; and the CO_2 capture level is regulated by the lean solvent flowrate [16].

Flue gas flowrate variation in the upstream power plant is considered as a main disturbance to the PCC process. To better accommodate the influence of flue gas, Posch and Haider [17] altered the general control structure by keeping the ratio between lean solvent flowrate and flue gas flowrate (L/G ratio) constant. Lin et al. [18] considered the hydraulic stability of the absorber and stripper. They proposed to maintain the solvent flowrate constant and adjust the CO_2 capture level via manipulating the re-boiler steam flowrate. Other works conducted relative gain array (RGA) analysis to quantify the correlations among key variables within the PCC system. The controlled variables (CV) and manipulated variables (MV) with minimal influences on other control loops were paired together [19].

Besides the conventional single-loop based controllers, developing advanced controllers is another key research area for the flexible control of the solvent-based PCC. Because the PCC process is characterized by slow response and strong couplings among multi-variables, model predictive controller (MPC) has received much attention [20]. By using a dynamic model to estimate the future response of the PCC system under candidate control sequences, MPC can find the optimal control actions for desired capture level tracking [21], flue gas disturbance rejection [22] and even the best economic performance [23]. A critical review of the recent dynamic modelling, system identification and control of the solvent-based PCC processes was provided in [10].

However, these studies only focused on the standalone PCC process only. Although the variation of flue gas caused by the FFFPS load change has been analyzed, the dynamic influence of PCC operation on the FFFPS was not considered. As the operation of PCC requires large amount of heat for solvent regeneration, plenty of steam is extracted from the turbine and fed to the re-boiler, which can reduce the FFFPS power generation up to 10% [24]. The use of re-boiler steam will also influence the load ramping speed of FFFPS. For example, in case of FFFPS load increase, more steam must be used in the PCC re-boiler to handle more flue gas generated from the upstream plant. However, such an operation is in direct conflict with the load increase demand of the FFFPS, which will slow down the load ramping speed and reduce the flexibility of FFFPS that is reserved for renewable energy accommodation. A report from IEA GHG [25] has recommended that developing dynamic models and investigating the transient characteristics of the integrated FFFPS-PCC process should be included in future studies to collaborate the operation of FFFPS and PCC.

Lawal et al. [26] carried out dynamic simulations of a 500MWe subcritical CFPP-PCC plant model, where independent PI controllers were implemented in the model for the adjustment of power output and CO_2 capture level. Their simulations illustrated that the response speed of PCC is much slower than that of the CFPP. Nevertheless, the interactions between the CFPP and PCC were not considered in their control design. Consequently, significant fluctuations appeared during the simulation. Montañés et al. [27] developed dynamic model for a commercial-scale combined cycle gas turbine (CCGT) plant equipped with monoethanol amine (MEA)-based PCC process. Operating performance of the PCC plant under five different control strategies was tested in cases of gas turbine load changes and the impact of PCC operation on the steam turbine power output was also analyzed. However, their study did not point out a suitable control strategy for the combined CCGT-PCC system to actively handle the interactions between the two plants.

Wu et al. [28] characterized the dynamic behavior of the integrated CFPP-PCC plant and developed a centralized predictive

controller to achieve a coordinated regulation of the power output and CO_2 capture level. A trade-off between power generation and carbon emission abatement could easily be attained by changing the weighting matrix of the MPC. They further developed two MPCs for the CFPP and PCC respectively in [29], where the two MPCs were closely linked through continuous exchange of predicted flue gas and re-boiler steam information. Three operation modes were then presented for the integrated CFPP-PCC plant to fully exert its functions in grid power regulation and CO_2 reduction. However, none of these studies sufficiently considered the distinct dynamics and operating requirements of the CFPP and PCC in the control system design.

In fact, although the steam drawn-off from turbine to re-boiler has crucial effects on both the FFFPS and PCC systems, the effects are not at the same time scale. Fig. 1 shows the responses of power output and CO_2 capture level corresponding to a 10% re-boiler steam flowrate reduction in a 660MWe CFPP-PCC plant model. Noticeable distinction can be observed that the power plant finishes the transition and enters new steady-state in about 1 minute, while long settling time in the scale of hundred minutes is required for the PCC. That is to say, the effect of re-boiler steam change on the PCC has not yet begun, but its effect on the FFFPS has already ended. This feature allows the PCC to be used as an energy storage device, which can quickly store/release additional energy for FFFPS by changing the re-boiler steam flowrate.

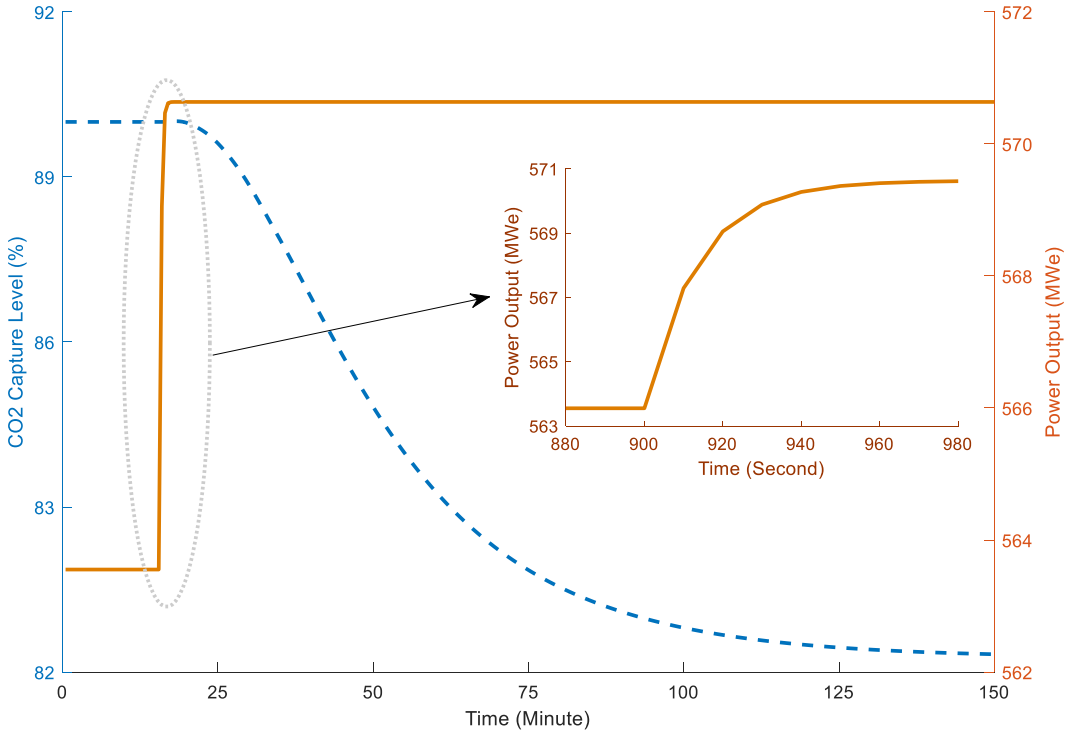

Fig. 1. Responses of power output and CO_2 capture level corresponding to a 10% re-boiler steam flowrate reduction in a 660MWe CFPP-PCC plant model (red solid line: power output; blue dashed line: CO_2 capture level).

On the other hand, the operational requirements for the FFFPS and PCC are also quite different. The FFFPS are expected to change the power output as fast as possible, so that more fluctuating renewable energy can be integrated into the grid. Prompt load change is thus as important as the reduction of CO_2 emission in the entire power system. However, the control requirements of the PCC system for a given CO_2 capture level are much more relaxed, because the carbon emissions are not considered to have an immediate impact on the environment.

Considering these, this paper proposes a novel operation strategy for the integrated FFFPS-PCC system, where a priori manipulation of the re-boiler flowrate is given to the FFFPS load change. The PCC is thus operating as an energy storage device, which can adjust the charging rate continually during the FFFPS load following, providing the plant with additional flexibility. Two MPCs are then designed for the FFFPS and PCC plants respectively. The simulations on a 660MWe supercritical CFPP-PCC model demonstrate that the developed collaborative control system can effectively improve the load-following ability of the power plant with little impact on the PCC operation. The main novelties of this paper are:

1) A novel control strategy for the integrated CFPP-PCC system is proposed using collaborative predictive controllers;

2) The distinct dynamics and operating requirements of the CFPP and PCC systems are fully utilized in the collaborative

control system design, leading to an effective control strategy;

3) The PCC is exploited as an energy storage device under the proposed collaborative predictive control system, which can quickly store/release extra energy for the CFPP in addition to the primary function of carbon emission reduction.

The rest of the paper is organized as follows: Section 2 briefly describes the 660MWe CFPP-PCC model used in this study. Section 3 presents the collaborative control strategy developed for the CFPP-PCC system based on the MPC technique. Simulation results are given in Section 4, where different operation schemes for the CFPP and PCC are tested and compared with other controllers for their performance in power plant load following and CO_2 reduction being assessed. Conclusions are drawn in Section 5.

2. System Description

The plant under consideration in this paper is a 660MWe supercritical CFPP integrated with 30% MEA-based PCC process, which is shown in Fig. 2. The CFPP model was developed based on a hybrid modelling approach, which fuses the physics-based understanding of the process and the information contained in the real-time operation data to develop a satisfactory process model [30]. The hybrid modelling approach can be divided into two steps. In the first step, we use first-principle approaches, such as conservation of mass, energy and momentum to develop the model framework of the main equipment in the supercritical CFPP (for example, the coal pulverizing system, steam generator system, turbine system, flue gas system), whose working mechanism has been thoroughly understood. Then the remaining unknown/unclear parameters of the CFPP model, for example, the heat and mass transfer coefficients, rely on the historical data of the plant. Particle swarm optimization (PSO) algorithm, which is a powerful machine leaning technique is explored for the parameter identification of this model. The CFPP model has been validated via steady-state and dynamic operational data archived from a 660MWe supercritical CFPP located in Anhui, China and has been shown to reflect the key dynamics of the CFPP satisfactorily [30].

A commercial software, gCCS®, is employed for the PCC model development to provide high-fidelity simulations of the CO_2 capture process [31]. The software gCCS® builds dynamic rate-based models of the absorber and stripper based on two film theory. The absorber/stripper model is distributed in the axial direction. The chemical reactions between solvent and CO_2 are assumed to occur only in the liquid film. Phase and chemical equilibrium is assumed to establish at the interface [31]. The PCC dynamic model in this study was developed based on a pilot-scale reference model [32], which has been validated through experimental data collected from the Separations Research Program (SRP) pilot plant in the University of Texas at Austin. This model was then scaled up in our previous works [30, 33] using the generalized pressure drop principle to deal with the flue gas from a 660MW CFPP and provide convincible simulations of the industrial-scale PCC process. Three absorbers are used in the PCC design. We assumed that the flue gas and lean solvent are equally distributed to the three absorbers. Detailed information of the CFPP-PCC model can be found in [30], thus it is not repeated here.

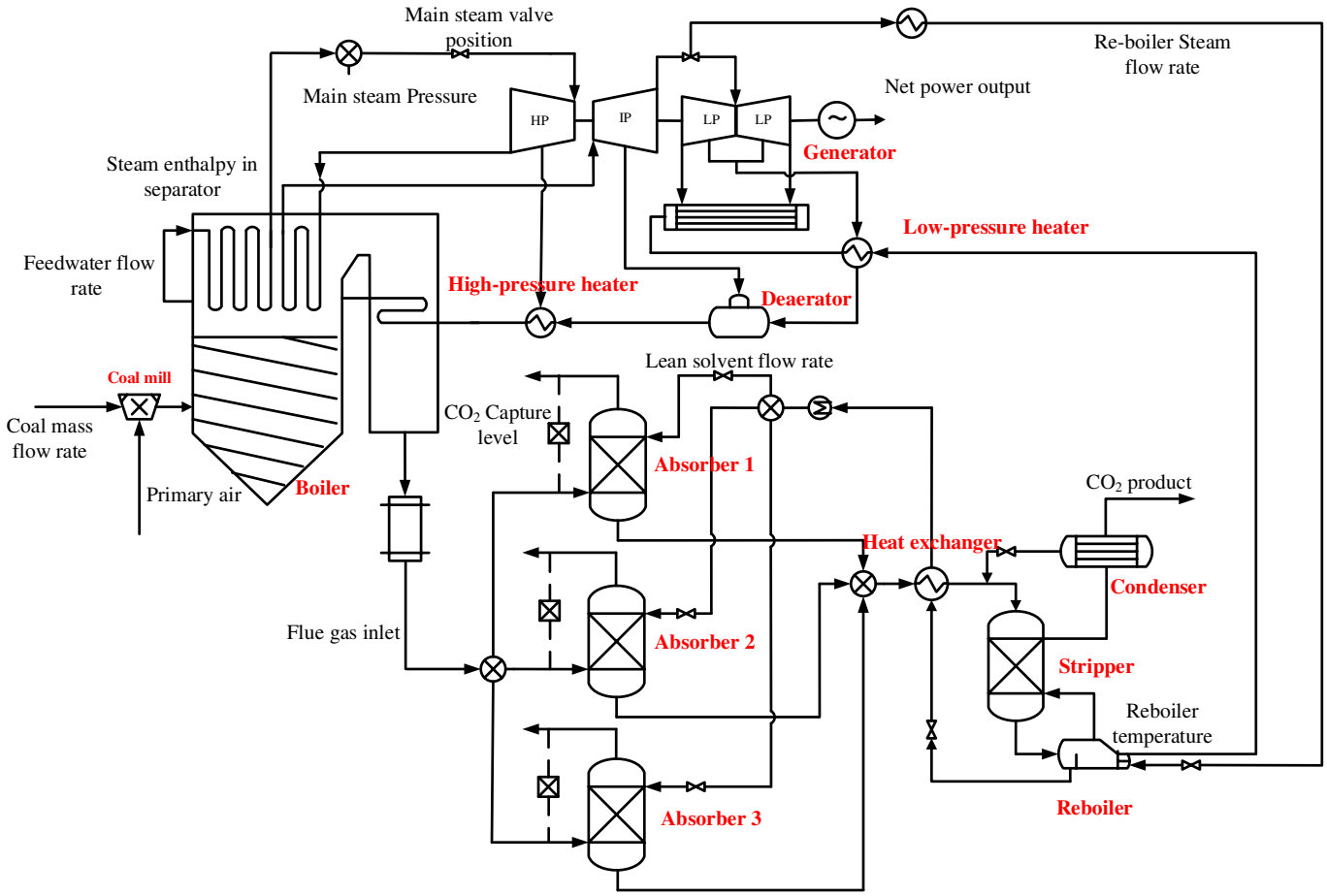

Fig. 2. Schematic diagram of the 660MWe supercritical CFPP-PCC process [30].

The feasible operation region of the CFPP retrofitted by the PCC is given in Fig. 3, where the coupling relationship between re-boiler steam flow and power output is illustrated. Line 1-2 presents the operation region of the original CFPP (without integration of the PCC), from turbine maximum continuous rating (TMCR) condition to 50% turbine heat consumption rate acceptance (THA) condition. After retrofitting to add the PCC, the operation of the PCC requires to extract steam from the intermediate-pressure/low-pressure (IP/LP) crossover of the steam turbine to the re-boiler for solvent regeneration. Consequently, the power output of the CFPP decreased as the re-boiler steam flow rate increases (See line 1-A-I-II-B for the TMCR condition and line 2-E-IV-III-D for the 50% THA condition). Lines A-E and B-C represent the minimum and maximum re-boiler steam flow rate conditions. Lines I-IV and II-III represent the 50% and 90% CO_2 capture level conditions of the integrated CFPP-PCC system. Line D-C represents the minimum LP turbine steam flow rate condition for the operation safety of the LP turbine. In such a condition, the increase of re-boiler steam flow rate can only be achieved by increasing the steam generated by the boiler to guarantee a lowest amount of steam being fed into the LP turbine. The main operating parameters of the corner points are listed in Table 1.

The integration of PCC unit enlarges the power regulation region of the CFPP. It can be observed from Fig. 3 that the feasible power adjustment region is extended from 360 MWe of the original plant (1-2) to 402.64 MWe after the PCC retrofitting (A-D). Meanwhile, by altering the re-boiler steam flowrate, a prompt change of around 10% current power load can be achieved for the CFPP. These findings reveal that a deeper and faster load regulation performance can be expected for the integrated CFPP-PCC plant.

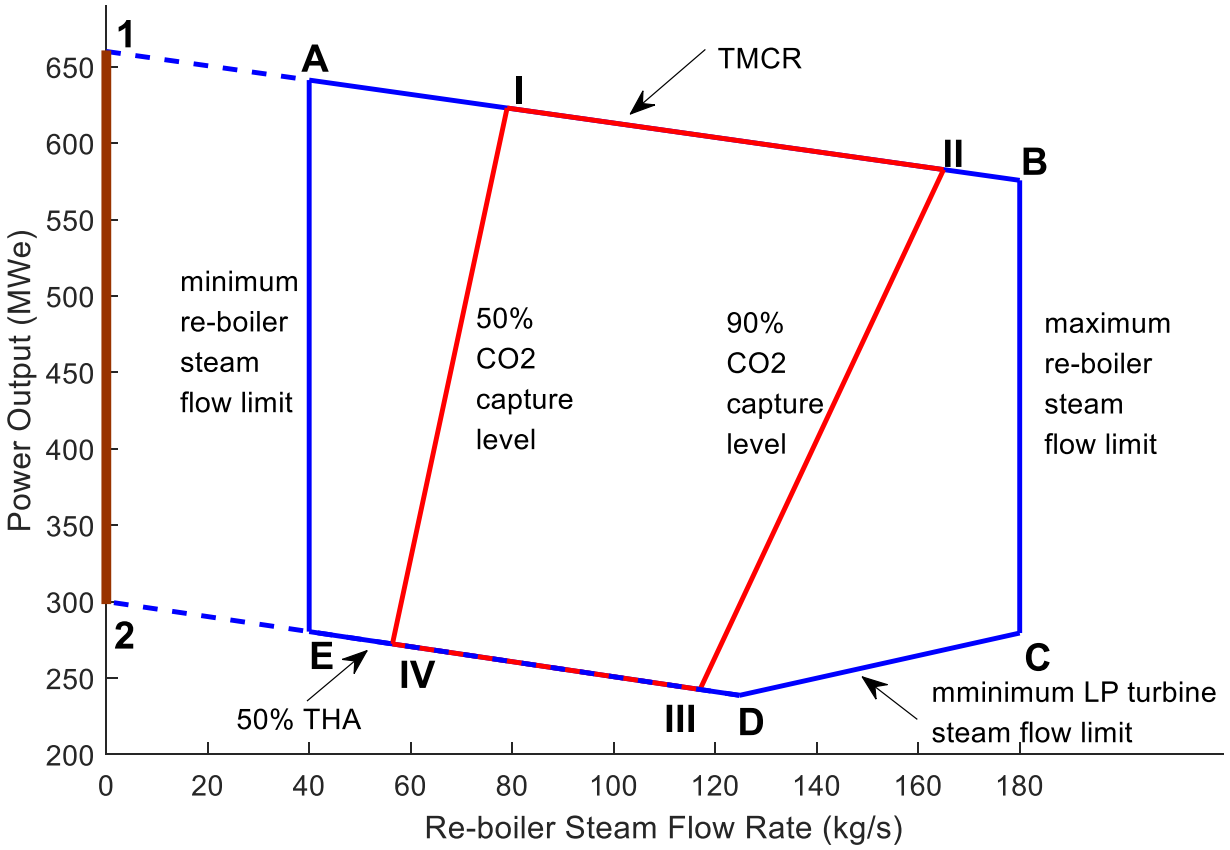

Fig.3. Feasible operation region of the retrofitted CFPP.

Table 1. Main operating parameters of the corner point of the retrofitted CFPP

	Coal mass flowrate (kg/s)	Feedwater flowrate (kg/s)	Main steam valve position (%)	Re-boiler steam flowrate (kg/s)	Power output (MWe)	Main steam pressure (MPa)	Steam enthalpy in separator (kJ/kg)	Flue gas flowrate (kg/s)
#1	75.29	544.41	98.11	/	660	24.84	2674.49	556.06
#2	34.22	233.67	83.36	/	300	14.20	2774.77	243.90
#A	75.29	544.41	98.11	40	641.26	24.84	2674.49	556.06
#B	75.29	544.41	98.11	180	575.63	24.84	2674.49	556.06
#C	41.88	288.88	86.60	180	279.40	16.29	2756.49	426.56
#D	34.22	233.67	83.36	124.80	238.62	14.20	2774.77	396.89
#E	34.22	233.67	83.36	40	280.33	14.20	2774.77	396.89
#I	75.29	544.41	98.11	79	622.98	24.84	2674.49	556.06
#II	75.29	544.41	98.11	165	582.67	24.84	2674.49	556.06
#III	34.22	233.67	83.36	117	242.45	14.20	2774.77	396.89
#IV	34.22	233.67	83.36	56.4	272.26	14.20	2774.77	396.89

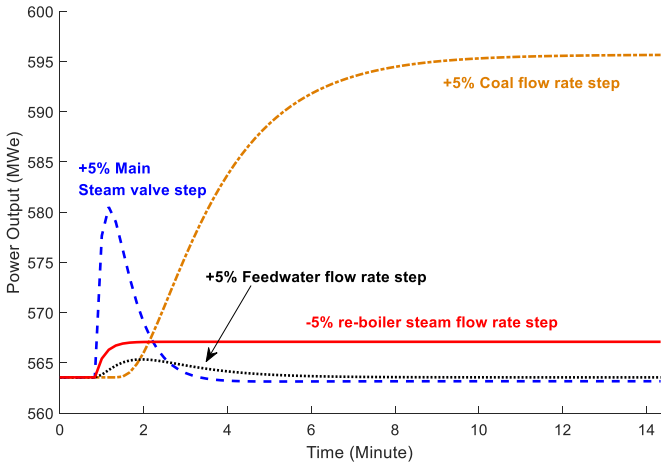

Fig. 4. Responses of power output corresponding to the step changes of key variables.

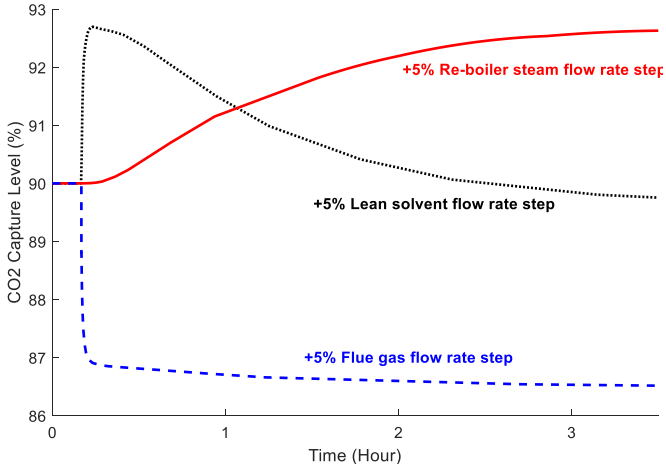

Fig. 5. Responses of CO_2 capture level corresponding to the step changes of key variables.

We further investigate the dynamic performance of the CFPP and PCC processes. The responses of power output in cases of key MV step changes are illustrated in Fig. 4. It can be observed that the coal flowrate has the biggest influence on the power output but is relatively slow. It takes around 9 minutes for the power output to enter new steady-state after the coal flowrate changes, including around 40 seconds of pure delay in the initial stage of the response. Therefore, it is difficult to achieve a flexible control of the power output depending on manipulating the coal flowrate only. The reason for this feature lies in the time consumed by the coal pulverizing, delivering, combustion and heat transfer to the water/steam. Regarding the turbine steam valve, its influence on the power output is strong and fast, because the heat generated in the boiler is quickly released or stored by the regulation of steam valve [6]. Nevertheless, such an influence is temporary and can easily cause a strong variation of main steam pressure. Thus, the changing rate of the steam valve cannot be too large for the safe operation of the power plant. The influence of feedwater flowrate is relatively small, which has the similar quick and temporary feature like the influence of steam valve. The change of water supply is easy to cause the fluctuation of steam temperature; thus, it is usually manipulated in consistent with the coal flowrate. Apart from the three aforementioned MVs, regulating the re-boiler steam flow rate can achieve a permanent adjustment of the power output in less than 1 minute; moreover, since the re-boiler steam is withdrawn at the crossover of IP/LP turbine, it gives little impact on the main steam pressure and temperature.

On the other hand, the influence of re-boiler steam flow rate on the solvent-based PCC process is much slower as shown in Fig. 5. It takes more than 2 hours for the CO_2 capture level to stabilize in case of a step change of re-boiler steam flowrate. In contrast, the adjustment of lean solvent flowrate is more effective, which can alter the capture level in around 3-4 minutes. The capture level will then slowly return to the previous level, because the increase of lean solvent flowrate will reduce the re-boiler temperature, leading to an increase in lean solvent loading. The significant influence of the flue gas flowrate on the CO_2 capture level is also illustrated in Fig. 5. The capture level changes immediately as the flue gas flowrate changes considering the definition of the capture level:

$$\mathrm{CO_2\ Capture\ Level} = \frac{\mathrm{CO_2}\ \textit{in the flue gas} - \mathrm{CO_2}\ \textit{in the clean gas}}{\mathrm{CO_2}\ \textit{in the flue gas}} \tag{1}$$

The behavior analysis shows the dynamic interactions between the CFPP and PCC plants, it also provides us an important insight for the controller design of the integrated CFPP-PCC process. The re-boiler steam flow can be “borrowed” from the PCC system to assist the load regulation of CFPP. It can then be “returned” after the load regulation is almost finished. Since the influence of steam on the PCC is much slower than that on the CFPP, we can alleviate the influence during this period by adjusting the lean solvent flowrate. Motivated by these findings, we propose a novel collaborative control scheme for the integrated CFPP-PCC system, which aims to explore the function of PCC to improve the flexibility of the CFPP in addition to the primary function of carbon emission reduction.

3. Collaborative Predictive Control of the Integrated CFPP-PCC unit

Fig. 6 gives the schematic diagram of the proposed collaborative control system for the integrated CFPP-PCC process, which is composed by three parts: the CFPP controller, the PCC controller and the CFPP target calculator.

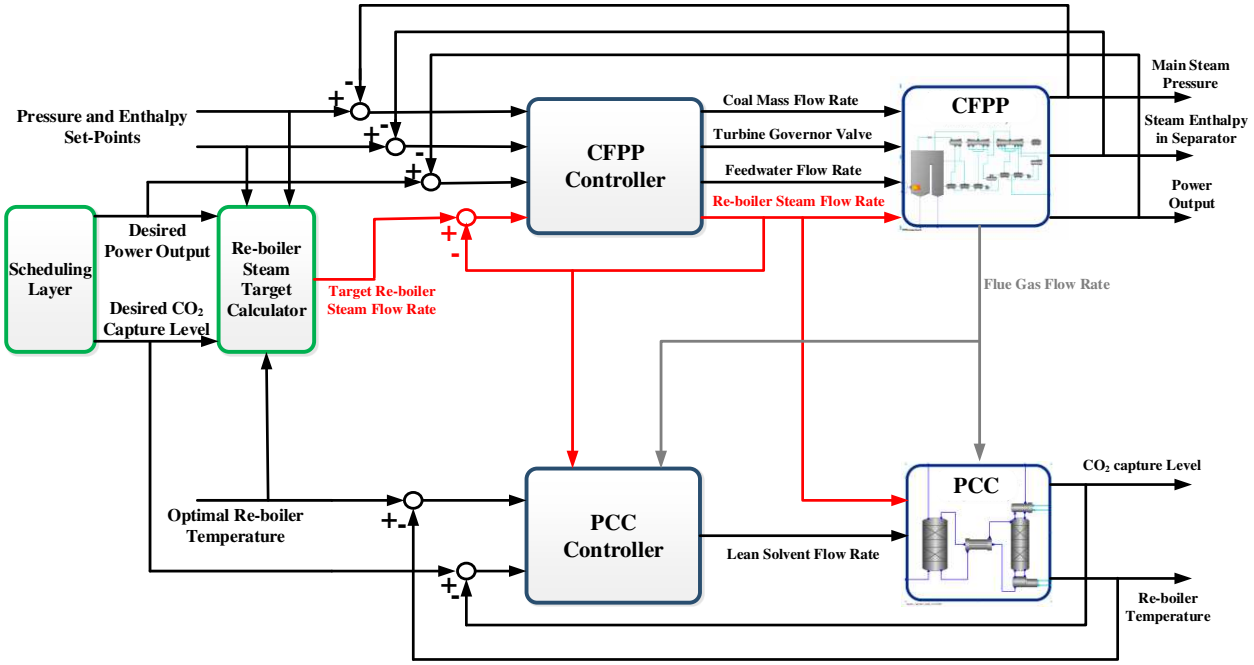

Fig. 6. Schematic diagram of the proposed collaborative control system for the integrated CFPP-PCC process.

A. CFPP controller design

The CFPP controller is responsible for the adjustment of core variables in the CFPP. It drives the plant to track the desired power output (y_1) set-point while maintaining the main steam pressure (y_2) and separator steam enthalpy (y_3) at given levels by manipulating the coal flowrate (u_1), main steam valve (u_2) and feedwater flowrate (u_3). On this basis, the re-boiler steam flow rate (u_4) is considered as an auxiliary MV in the CFPP control system design to accelerate the load ramping of the plant.

The approach of model predictive control (MPC) is used for the control of the CFPP, which has been found to provide superior regulating performance, especially for the multi-variable, constrained and slow response processes [34]. An objective function (2) is considered in the MPC design to complete the regulation task of the CFPP:

$$\begin{aligned} J_{CFPP}(k) = &\sum_{N=0}^{N_y} (y_{CFPP}(k+N\,|\,k) - r_{CFPP}(k+N))^T Q_{CFPP} (y_{CFPP}(k+N\,|\,k) - r_{CFPP}(k+N)) \\ &+ \sum_{N=0}^{N_u} \Delta u_{CFPP}(k+N)^T R_{CFPP} \Delta u_{CFPP}(k+N) + S \sum_{N=0}^{N_u} (u_4(k+N) - T)^2 \end{aligned} \tag{2}$$

The first term of the objective function represents the tracking performance of the CVs, where $y_{CFPP}(k+N|k)$= [$y_1(k+N|k)$, $y_2(k+N|k)$, $y_3(k+N|k)$]$^{\mathrm{T}}$ is the prediction of future CVs of the CFPP at time instant $k+N$ based on the candidate control sequences given at current time instant k, and $r_{CFPP}(k+N)$ is the future set-points for the CVs. The second term takes account of the variation of the MVs for the smooth operation of the plant, in which $\Delta u_{CFPP}(k+N)$=[$\Delta u_1(k+N)$, $\Delta u_2(k+N)$, $\Delta u_3(k+N)$, $\Delta u_4(k+N)$]$^{\mathrm{T}}$ is the increments of the CFPP MVs at time instance $k+N$. The last term considers the carbon capture target of the integrated plant, where T is the re-boiler steam flow rate required for the PCC to achieve the expected CO_2 capture level; N_y and N_u are the predictive and control horizons of the MPC; and Q_{CFPP}, R_{CFPP}, S are the weighting parameters to adjust the preference of these three terms in the objective function. By setting a small value of S, the control idea of this paper can be easily achieved that the MPC will manipulate the re-boiler steam flowrate first for the CFPP load regulation and gradually drive it to the given value T for CO_2 capture when the load regulation is almost finished.

A state space model (3) is developed as the predictive model to estimate the values of future CVs corresponding to the candidate future MV sequences:

$$\begin{cases} x_{CFPP}(k+1|k) = Ax_{CFPP}(k|k) + Bu_{CFPP}(k) \\ y_{CFPP}(k|k) = Cx_{CFPP}(k|k) + Du_{CFPP}(k) \end{cases} \tag{3}$$

where x_{CFPP} is the state vector of the CFPP predictive model; A, B, C, D are the model parameters. It should be noted that, since the re-boiler steam flowrate has been actively incorporated into the CFPP control instead of passive treating it as a disturbance, the influence of re-boiler steam on the operation control of CFPP will be transformed from "harmful" to "useful." Smooth operation of CFPP can thus be expected under the proposed control strategy.

Model (3) can be identified through subspace identification [35] based on the input-output data of the CFPP plant. At each sampling time, by minimizing the objective function (2) subject to the predictive model (3) and the operating constraints (4) due to the physical limitations of the actuators,

$$\begin{aligned} u_{CFPP}^{\min} \le u_{CFPP} \le u_{CFPP}^{\max} \\ \Delta u_{CFPP}^{\min} \le \Delta u_{CFPP} \le \Delta u_{CFPP}^{\max} \end{aligned} \tag{4}$$

the best control sequence for the CFPP operation can be calculated by the MPC. Detailed algorithm of the MPC is similar to that given in [28], thus is not repeated here.

B. PCC controller design

The PCC controller is designed to control the CO_2 capture level (y_4) and re-boiler temperature (y_5), which are two key variables in the solvent-based PCC process [16, 26]. Because the re-boiler steam flowrate (u_4) has been manipulated to accelerate the CFPP load change, the lean solvent flowrate (u_5) becomes the only available MV in the PCC controller during this period. It must be manipulated properly so that the PCC system can attain desired capture level and re-boiler temperature as much as possible.

We also propose to use the MPC for the PCC controller design, in which the following objective function is considered:

$$\begin{aligned} J_{PCC}(k) = &\sum_{N=0}^{N_p} (y_{PCC}(k+N|k) - r_{PCC}(k+N))^T Q_{PCC} (y_{PCC}(k+N|k) - r_{PCC}(k+N)) \\ &+ \sum_{N=0}^{N_c} \Delta u_5(k+N)^T R_{PCC} \Delta u_5(k+N) \end{aligned} \tag{5}$$

where $y_{PCC}(k+N|k) = [y_4(k+N|k), y_5(k+N|k)]^{\mathrm{T}}$ is the prediction of future CVs of the PCC at time instant $k+N$ based on the candidate control sequences and disturbances given at current time instant k; $r_{PCC}(k+N)$ is the future set-points for the CVs; $\Delta u_5(k+N)$ is the increments of the lean solvent flowrate at time instance $k+N$; N_p and N_c are the predictive and control horizons, respectively. Noting that using one MV to adjust two CVs is a difficult task, the weighting parameters Q_{PCC} and R_{PCC} should be set carefully according to the control preferences.

State-space model is identified and used as the predictive model to estimate the values of future CVs in the PCC process:

$$\begin{cases} x_{PCC}(k+1|k) = A^* x_{PCC}(k|k) + B^* u_5(k) + E^* d(k) \\ y_{PCC}(k|k) = C^* x_{PCC}(k|k) + D^* u_5(k) + F^* d(k) \end{cases} \tag{6}$$

In model (6), $d(k) = [u_4(k), f(k)]^{\mathrm{T}}$ is the disturbance to the PCC system, including the re-boiler steam flow rate u_4 and flue gas flow rate f, which two can be provided by the CFPP controller; x_{PCC} is the state vector of the PCC predictive model; and A^*, B^*, C^*, D^*, E^*, F^* are the model parameters.

The following constraints are set in the PCC MPC development considering the magnitude and rate limitations of the lean solvent flowrate and the requirement of the re-boiler temperature for safe operation.

$$\begin{aligned} u_5^{\min} \le u_5 \le u_5^{\max} \\ \Delta u_5^{\min} \le \Delta u_5 \le \Delta u_5^{\max} \\ y_5^{\min} \le y_5 \le y_5^{\max} \end{aligned} \tag{7}$$

At each sampling time, by minimizing the objective function (5) subject to the predictive model (6) and the operating constraints (7), the best lean solvent flow rate can be calculated by the MPC and implemented in the PCC process.

C. Re-boiler steam target calculator design

The target calculator is then developed for the collaborative operation of the CFPP controller and PCC controller, which will calculate the re-boiler steam flowrate required by the PCC according to the desired power output and CO_2 capture level. The CFPP controller will alter the re-boiler steam flowrate to this value once the load regulation is almost finished, so that the carbon capture requirement can be met.

An inverse artificial neural network model is identified for the integrated CFPP-PCC system [30] and used in the re-boiler steam target calculator, which will estimate the target re-boiler steam flowrate T based on the desired power output, CO_2 capture level and the set-points of steam pressure, enthalpy and re-boiler temperature.

4. Simulation Results

The transient performance of the CFPP-PCC system under different operating and control strategies is shown in this section. Power output and capture level set-points changes are considered in the simulation to represent the operation condition of the integrated plant. We assume that at t=5min, the CFPP participates the load regulation of the grid and the power output set-point rises from 432.9MWe to 552.8MWe. The CFPP is operated under the sliding pressure mode that the main steam pressure set-point changes from 21.4MPa to 24.8MPa, and the separator steam enthalpy changes from 2722.1kJ/kg to 2674.5 kJ/kg. The CO_2 capture level set-point remains the same at 90% during the CFPP load increase. Then at t=102.5min, the power output set-point decreases to 506.9MWe. Corresponding to this change, the steam pressure and enthalpy set-points change to 24MPa and 2702.5kJ/kg, respectively, and the CO_2 capture level set-point also decreases to 70%. The re-boiler temperature set-point is fixed constant at 392.2K, which is the optimal re-boiler temperature of this PCC plant.

The following parameters are set for the CFPP and PCC controllers:

MPC for CFPP control: the sampling time T_s is set to 10s; the predictive and control horizons are set as N_y=20, N_u=5. The weighting parameters are set as Q_{CFPP}=*diag*(80, 150, 1) considering the need for fast load regulation and smooth change of main steam pressure; R_{CFPP} is set to *diag*(30, 5×10^6, 5, 10) to avoid the drastic variation of the actuators, especially the turbine governor valve; S is set to 1, so that the priority of manipulating the re-boiler steam flow rate is given to the CFPP control. The operating constraints are set as: $u_{CFPP}^{\min}=\left[30,\ 0.75,\ 220,\ 40\right]^T$, $u_{CFPP}^{\max}=\left[80,\ 1,\ 560,\ 180\right]^T$, $\Delta u_{CFPP}^{\min}=\left[-1,\ -0.007,\ -10,\ -3.33\right]^T$, $\Delta u_{CFPP}^{\max}=\left[1,\ 0.007,\ 10,\ 3.33\right]^T$.

MPC for PCC control: the sampling time T_s is set to 30s, the predictive and control horizons are set as N_p=20, N_c=5. The weighting parameters are set as Q_{PCC}=*diag*(2×10^5, 1) since tracking the desired CO_2 capture level is regarded as the primary task of the PCC; R_{CFPP} is set to 1. The operating constraints are set as: $u_5^{\min}=250$, $u_5^{\max}=700$, $\Delta u_5^{\min}=-20$, $\Delta u_5^{\max}=20$, $y_5^{\min}=383$, $y_5^{\max}=395$. The lean solvent flowrates given in this section refer to the flowrate values sent into each absorber.

4.1 Performance of the CFPP-PCC system under proposed collaborative control strategy

The transient performance of the CFPP under the proposed collaborative control strategy is shown in Figs. 7 and 8. Taking the load rising scenario as an example, when the load rising command is given to the CFPP, the proposed MPC quickly reduces the steam flowrate sent to the re-boiler. This part of steam can thus continue to expand in the LP turbine to generate more power. Meanwhile, the MPC increases the coal mass and feedwater flowrates to increase the steam generation in the boiler; and increases the main steam valve to drive more steam into the turbine. The power output is thus risen rapidly, which achieves the desired value in about 4.5 minutes. The increase of main steam valve and feedwater flowrate leads to the drop of steam pressure and enthalpy. The MPC begins to consider the adjustment of these two CVs and the operation of PCC system when the load tracking task is almost finished. We can observe in Fig. 7 that the main steam pressure and separator steam enthalpy are smoothly regulated to the set-points after certain levels of deviations. As the rise of load increases the flue gas flowrate, more re-boiler steam is required to maintain a given capture level, the re-boiler steam flowrate is gradually recovered to the target value for CO_2 capture as illustrated in Fig. 8.

To demonstrate the effectiveness of the proposed collaborative control approach, the performance of three other operating strategies is also simulated for comparison:

A. Same collaborative control system with weight parameter S set to 10^6. According to the objective function (2), when S is set to a large value, the re-boiler steam will not be used for CFPP control, instead, it will be immediately manipulated to the required value for CO_2 capture.

B. Model predictive control of the standalone CFPP without the integration of PCC system. Except that there is no impact from re-boiler steam, the predictive model and parameters of this controller are the same as the proposed MPC for CFPP.

C. Conventional single-input single-output PI control of the CFPP-PCC system [26]. Boiler following mode is adopted for the CFPP control, which uses the coal mass flowrate, main steam valve and feedwater flowrate to control the main steam pressure, power output and separator enthalpy, respectively. For the PCC control, lean solvent flowrate is used to control the CO_2 capture level and the re-boiler steam flowrate is manipulated to control the re-boiler temperature. The PI parameters are set as: k_{P_pressure}= 2.0445, k_{I_pressure}= 0.04211; k_{P_enthalpy}= -0.083, k_{I_enthalpy}= -0.00463; k_{P_power}= 5.112e^{-04}, k_{I_power}= 2.045e^{-06}; k_{P_co2}= 162.34, k_{I_co2}= 8.729; k_{P_temp}= 650.131, k_{I_temp}= 6.269.

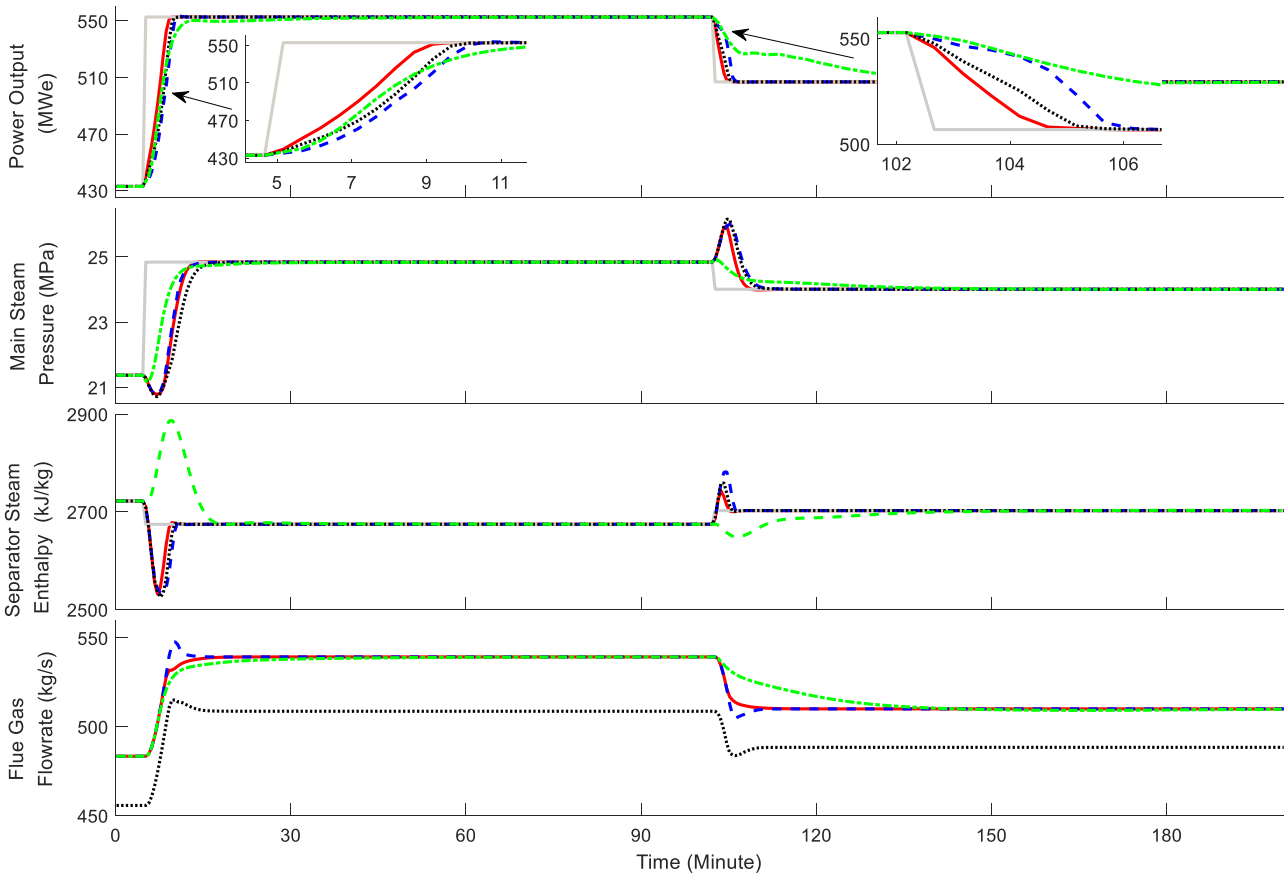

Fig. 7. Operating performance of the CFPP (CVs): red solid line: proposed collaborative control with S=1; blue dashed line: proposed collaborative control with S=10^6; black dotted line: model predictive control of the standalone CFPP; dotted-dashed green line: conventional PI control; solid grey line: reference.

It can be seen from Figs. 7 and 8 that by using the re-boiler steam in the CFPP adjustment, the proposed collaborative controller can provide superior performance over the other three controllers. It has the fastest tracking speed for power output with acceptable fluctuations in coal mass flowrate, main steam valve and feedwater flowrate.

In contrast, the re-boiler steam will not be used for CFPP adjustment when S is setting to 10^6. Instead, the collaborative controller will manipulate it to the required value for PCC directly as shown in the lower figure of Fig. 8. The increase of re-boiler steam will therefore slow down the load ramping of the CFPP. However, since the manipulation of re-boiler steam flowrate is still considered in the CFPP control design rather than the conventional PCC control, the dynamic impact of PCC operation on the CFPP control can be naturally avoided and a smooth load following can still be achieved for the CFPP.

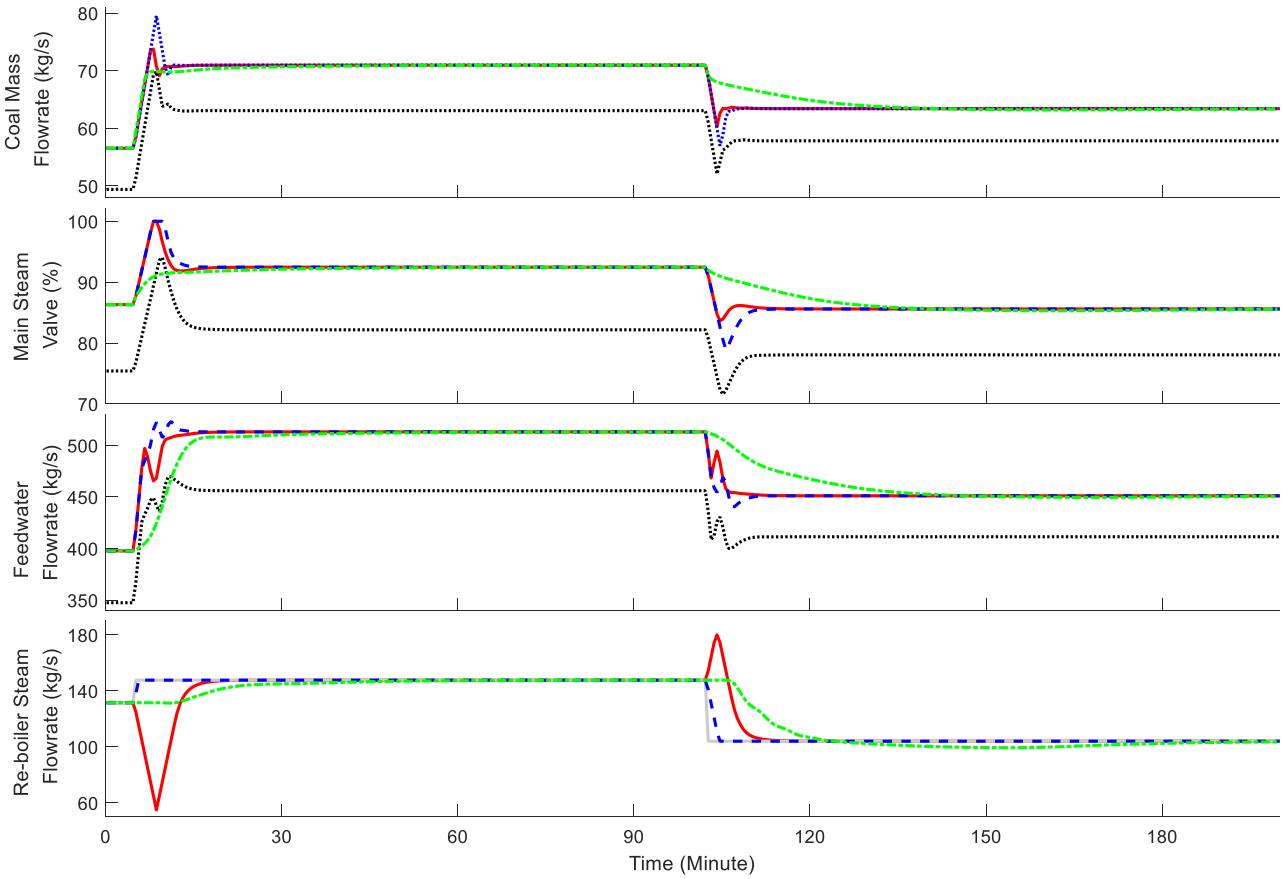

Fig. 8. Operating performance of the CFPP (MVs): red solid line: proposed collaborative control with S=1; blue dashed line: proposed collaborative control with S=10^6; black dotted line: model predictive control of the standalone CFPP; dotted-dashed gray line: re-boiler steam flow rate target.

For the conventional PI control, because both the power generation and carbon capture require to consume large amount of steam, and the re-boiler steam's impact on the CFPP operation is not taken into account in the control system, oscillations are easily appeared during the simulation, which has also been pointed out in [26]. For this reason, we must reduce the parameters of the controller, especially the power output controller to enhance the system stability. Consequently, the PI control system is much slower in power ramping compared with the collaborative MPCs. This feature is particularly prominent in the second stage of simulation, when both the set-points of power output and CO_2 capture level decrease at the same time. To reduce the power output, the CFPP control decreases the coal flow rate, leading to a drop in flue gas flowrate; and consequently, the CO_2 capture level gets increased and the capture level controller begins to decrease the lean solvent flowrate, which causes an increase in re-boiler temperature. As a result, the re-boiler temperature control reduces the steam flowrate to maintain the given temperature. However, such a control action further increases the power output, which is against the control target of the CFPP. Because the whole series of influences is very slow, the integration of PCC greatly degrades the load tracking performance of the CFPP under the conventional PI control system.

To evaluate the load ramping performance of the CFPP quantitatively, the regulation times T_r (s), ramping rates v (MWe/s) and integrated absolute errors IAE of the four operating strategies are calculated by (8)-(10) and listed in Table 2:

$$T_r = T_e - T_s \tag{8}$$

$$v = (N_e - N_s) / (T_e - T_s) \tag{9}$$

$$IAE = \int_{T_e}^{T_s} |e(t)|\, dt \tag{10}$$

where T_e and T_s are the end and start times of the regulation; N_e and N_s are the end and start power outputs; and $e(t)$ is the instantaneous tracking error of the power output. (End time refers the time control deviation has been minimized to 0.5% of the initial deviation)

The results in Table 2 clearly illustrate that the proposed collaborative control strategy can effectively accelerate the load ramping speed of the CFPP, shorten the transition period and minimize the tracking error. With the help of PCC re-boiler steam, the load ramping performance of the integrated CFPP-PCC plant can even be better than the standalone CFPP, and this advantage is more apparent in the case of small CFPP load change. The potential function of PCC to improve the flexibility of the CFPP is clearly demonstrated.

Table 2. Load ramping performance indexes of the CFPP

	Stage-1 (Load Increase)			
	proposed collaborative control (S=1)	collaborative control (S=10^6)	MPC of the standalone CFPP	conventional PI
T_r	270	370	310	1230
v	0.4332	0.3161	0.3773	0.0951
IAE	1.5956×10^4	2.3235×10^4	2.0517×10^4	2.6511×10^4
	Stage-2(Load Decrease)			
	proposed collaborative control (S=1)	collaborative control (S=10^6)	MPC of the standalone CFPP	conventional PI
T_r	180	230	210	3120
v	-0.2371	-0.1856	-0.2032	-0.0137
IAE	2.6886×10^3	6.1018×10^3	3.8491×10^3	3.274×10^4

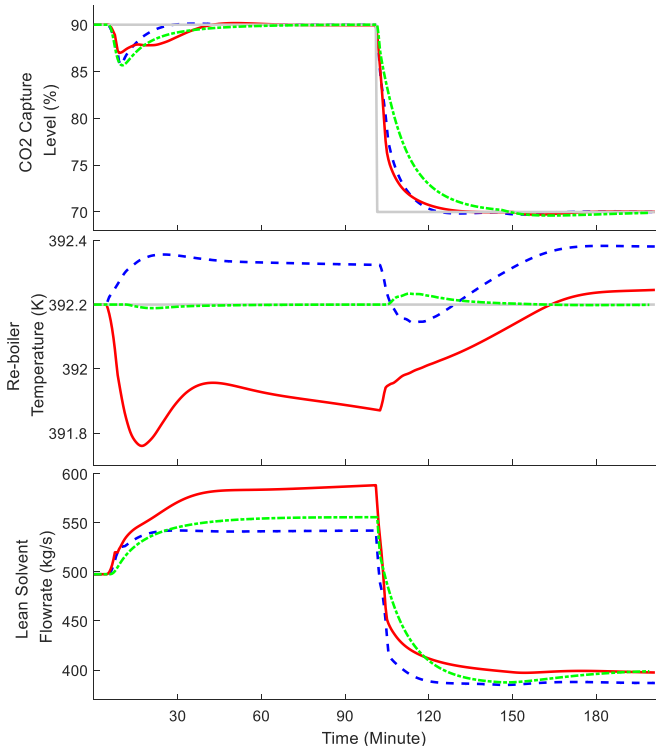

Fig. 9. Operating performance of the PCC (focus on CO_2 capture level control): red solid line: proposed collaborative control with S=1; blue dashed line: proposed collaborative control with S=10^6; dotted-dashed green line: conventional PI control; solid grey line: reference.

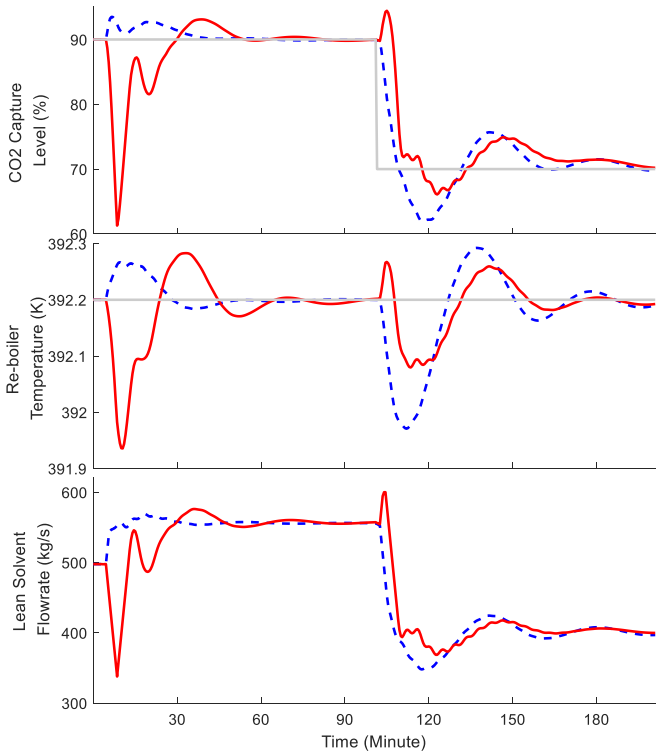

Fig. 10. Operating performance of the PCC (comprehensive control of CO_2 capture level and re-boiler temperature): red solid line: proposed collaborative control with S=1; blue dashed line: proposed collaborative control with S=10^6;solid grey line: reference.

We then show the operating performance of the PCC system in Fig. 9. For the proposed collaborative control strategy (S set to 1in the CFPP controller), strong disturbances occur for the PCC system from t=5min. The load rising of CFPP leads to a continued increase of flue gas flowrate and meanwhile, the re-boiler steam flowrate is rapidly decreased to assist the power plant load ramping. As a result, both the CO_2 capture level and re-boiler temperature decrease from the desired set-points. Since the

preference of PCC controller is given to the adjustment of the capture level, the lean solvent flowrate keeps increasing to drive the CO_2 capture level back to 90%. However, the increase of lean solvent flowrate will cause a further decrease in re-boiler temperature, and this situation is not relieved until the re-boiler steam flowrate is gradually increased to the target value. It requires 40 minutes for the capture level to return the set-point and a maximum deviation of 0.3℃ is appeared on the re-boiler temperature as shown in Fig. 9. For the second scenario starting at t=102.5min, the change of capture level set point leads to a sudden increase of the first term in the objective function (5). Meanwhile, the fast decrease of flue gas flowrate and the increase of re-boiler steam flowrate cause the rise of capture level, which further enlarge its deviation from the set-point. For this reason, the lean solvent flowrate is rapidly declined and the CO_2 capture level can be reduced to 70% in about 30 minutes.

For the collaborative control strategy with weight parameter S set to 10^6 in the CFPP controller, the operating performance on the PCC side is better. As the re-boiler steam is adjusted to the required value in time, the CO_2 capture level can approach the set-point faster with smaller variations in re-boiler temperature and lean solvent flowrate. Regarding the conventional PI controller, due to the error-based feedback characteristic, the adjustment performance of CO_2 capture level is worse than the MPCs, even the disturbance of flue gas flowrate is smoother. However, since the steam flowrate is only used for the re-boiler temperature control, the conventional PI control provides the best performance in re-boiler temperature. The regulation times T_r and *IAE* index of the capture level control for the two operating strategies are listed in Table 3. The comparisons show that, when re-boiler steam is manipulated for the CFPP load regulation, the operating performance of PCC is only slightly reduced compared with the collaborative MPC which manipulates the re-boiler steam only for the PCC control (S=10^6). Moreover, the capture level tracking performance of the PCC system under proposed collaborative MPC is still better than the conventional PI control, especially in the second stage of simulation, where both the CFPP load and CO_2 capture level are decreased.

Table 3. Control performance indexes of the PCC

	Stage-1 (Maintain Capture Level in Case of Load Increase)			**Stage-2 (Reduce Capture Level in Case of Load Decrease)**		
	proposed collaborative control (S=1)	collaborative control (S=10^6)	Conventional PI	proposed collaborative control (S=1)	collaborative control (S=10^6)	Conventional PI
T_r	2160	1380	2460	1740	1260	2580
IAE	3.3567×10^3	2.0328×10^3	3.9936×10^3	5.3011×10^3	5.6564×10^3	1.2336×10^4

Considering that 392.2K is the designed optimal re-boiler temperature, deviation from this temperature may decline the operation efficiency of the PCC system. We thus modify the parameter Q_{PCC} in the PCC controller to Q_{PCC} =$diag(7\times10^4, 2\times10^4)$ to attain a comprehensive adjustment of CO_2 capture level and re-boiler temperature. The simulation results are shown in Fig. 10.

We can find that for the proposed collaborative control strategy (S=1in the CFPP controller), the variation of the lean solvent flowrate is more significant compared with that in Fig. 9 in order to alleviate the effects of flue gas and re-boiler steam disturbances and balance the adjustments of capture level and re-boiler temperature. There are strong fluctuations on the CO_2 capture level, the maximum deviation reaches -28.7% for the load increase case, compared with less than -3% when only focused on the capture level control. The capture level can be slowly controlled to the set-points after the re-boiler steam flow rate returns to the required level, but the transition time is much longer than that shown in Fig. 9. Nevertheless, the performance of re-boiler temperature gets improved. The deviation becomes smaller and the designed optimal temperature can be achieved without offset. Fig. 9 also illustrate that the operating performance of the PCC system becomes better when weight parameter S in the collaborative controller is set to 10^6, especially in the load increase, CO_2 capture level fixed scenario.

The total amount of CO_2 captured m_{CO2}, steam consumption m_{steam} and steam consumption rate (steam consumption per unit of CO_2 captured) R_{steam} during the whole simulation are shown in Table 4. The conventional PI system is discovered to have the best economic performance since it provides the best re-boiler temperature control as illustrated in Fig. 9. However, the steam consumption rate of the proposed controller is only 0.8% worse. The comparison results also show that the steam consumption rate of the PCC system is slightly lower when both the CO_2 capture level and re-boiler temperature are considered in the PCC control. This control scheme can be recommended if achieving desired CO_2 capture level is not regarded as an urgent operational requirement.

Table 4. Environmental and economic performance of the PCC

	proposed collaborative control (S=1)		**collaborative control (S=10^6)**		**conventional PI**
	control of CO_2 capture level	control of CO_2 capture level and re-boiler temperature	control of CO_2 capture level	control of CO_2 capture level and re-boiler temperature	
m_{CO2} **(Ton)**	1093.8	1099.2	1095.8	1102.5	1101.0
m_{steam} **(Ton)**	1512.7	1512.7	1524.2	1524.2	1510.5
R_{steam}	1.383	1.376	1.391	1.382	1.372

The above simulations show that by incorporating the re-boiler steam flowrate into CFPP control, we can turn the adverse dynamic effect of PCC on CFPP control operation into benefit, accelerate the load ramping speed and improve the flexibility of the CFPP. The operation performance of the PCC has some degradation since the re-boiler steam is not directly participating in its adjustment. However, considering the control requirement for the CO_2 capture, this performance degradation is completely acceptable, especially when the desired capture level changes synchronously with the power load. Moreover, the improvement of CFPP load ramping performance can provide strong support for the integration of renewable energy into the grid. From this point of view, it can also contribute to the reduction of CO_2 emission.

4.2 Performance of the PCC under different control strategies

The simulations in Section 4.1 demonstrate the advantages of using the re-boiler steam in the CFPP load regulation. It also illustrates that when the re-boiler steam does not match the required value in short term, the PCC system is still able to achieve an acceptable operating control performance by manipulating the lean solvent flowrate only. Since the proposed MPC for PCC system is essentially a single variable controller, other conventional controllers suggested in open literatures may also attain satisfactory performance under the proposed collaborative operating strategy. For this reason, the performance of different PCC control approaches is tested in this section:

A. Constant lean solvent [18]: the lean solvent flow rate is fixed constant at 497.7kg/s throughout the simulation;

B. Constant L/G ratio [17]: the ratio of lean solvent flowrate to the flue gas flowrate (L/G ratio) is maintained at 3.0888 throughout the simulation. The lean solvent flowrate is manipulated according to the flue gas flowrate under this control mode;

C. PI temperature [19]: Conventional PI controller, which manipulates the lean solvent flow rate to control the re-boiler temperature (k_P=365.7, k_I=1.2);

D. PI capture level [16]: Conventional PI controller, which manipulates the lean solvent flow rate to control the CO_2 capture level (k_P=292.3, k_I=11.5).

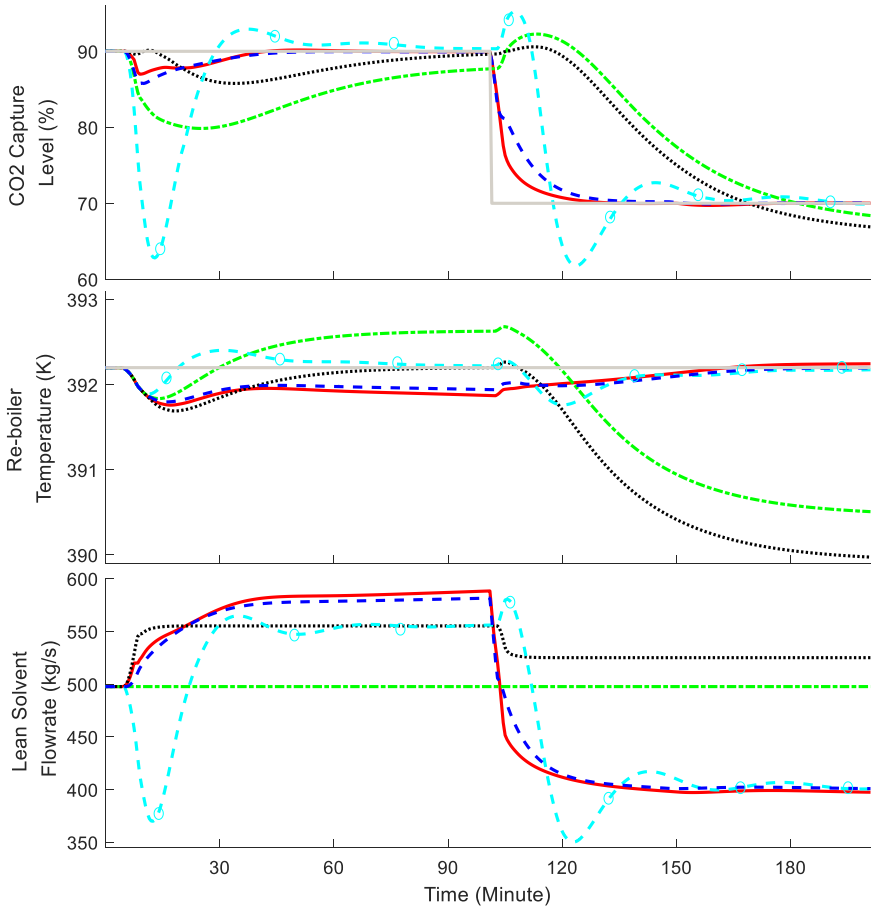

Fig. 11. Operating performance different PCC controllers under the proposed collaborative operating strategy: red solid line: proposed MPC; blue dashed line: PI capture level; circled lake blue dashed line: PI temperature; black dotted line: constant L/G ratio; green d dotted-dashed green line: constant lean solvent. grey dotted line: reference.

The simulation results of these controllers are shown in Fig. 11. Under the constant lean solvent mode, there are no adjustment actions implemented on the PCC system. The CO_2 capture level and re-boiler temperature deviate from the set-points under the disturbances of flue gas and re-boiler steam flowrates. Although the capture level starts to approach the set-point as the amount of re-boiler steam gradually returns to the required value, there is still an apparent deviation after a long transition time. The constant L/G ratio control shows a much better performance in the first stage of simulation when only the CFPP load demand change is considered. The CO_2 capture level is slowly controlled back to the desired value without large deviation; and the performance of re-boiler temperature is even better than that of the MPC. However, such a control strategy is not suitable for the case of CO_2 capture level change. Inadequate reduction of lean solvent flowrate results in a too high capture level and a too low re-boiler temperature, which can be discovered in Fig. 11 from t=102.5min. The PI temperature can well fulfill its design intent that the re-boiler temperature is maintained closely around the set-point throughout the simulation. However, because the impact of lean solvent is slow on the re-boiler temperature but fast on the capture level, strong fluctuations appeared on the CO_2 capture level and lean solvent flowrate. The PI capture level gives the best performance among the four test controllers, which can track the capture level set-point quickly without much deviations in re-boiler temperature. Its performance is even comparable to that of the MPC.

The *IAE* indices of the tested PCC controllers are listed in Table 5. It can be concluded from Fig. 11 and Table 5 that, the PI temperature, PI capture level and proposed MPC can all meet the flexible operation requirement of the PCC system in the condition that the re-boiler steam is manipulated for CFPP control in short term. Among them, control of the CO_2 capture level is found to be more effective than control of the re-boiler temperature. The fixed L/G ratio can also attain a satisfactory performance in case of CFPP load change, however, it is not suitable if the CO_2 capture level is required to be changed. The fixed lean solvent mode gives the worst performance, the desired capture level and re-boiler temperature cannot be maintained in the presence of flue gas and re-boiler steam disturbances. The proposed MPC can provide the best performance for the PCC system.

Table 5. Performance indexes for different PCC controllers under the proposed collaborative operating strategy

	Stage-1 (Maintain Capture Level in Case of Load Increase)		**Stage-2 (Reduce Capture Level in Case of Load Decrease)**	
	IAE for CO_2 capture level	***IAE for re-boiler temperature***	***IAE for CO_2 capture level***	***IAE for re-boiler temperature***
Fixed lean solvent	3.4259×10^4	1.7496×10^3	5.6596×10^4	6.4358×10^3
Fixed L/G ratio	1.1402×10^4	9.3076×10^2	5.0717×10^4	8.8166×10^3
PI temperature	2.4115×10^4	5.5347×10^2	2.6992×10^4	7.1976×10^2
PI capture level	4.0609×10^3	1.4529×10^3	8.9205×10^3	6.1955×10^2
proposed MPC	3.3567×10^3	1.7151×10^3	5.3011×10^3	5.9939×10^2

5. Conclusion

To overcome the flexible operating issues of the integrated CFPP-PCC system, this paper presents an in-depth study on the dynamic interactions between the CFPP and PCC plant. Simulation study of a 660MW supercritical CFPP model integrated with an MEA-based PCC has shown that the impact of re-boiler steam change on the power generation of CFPP is more than 100 times faster than that on the PCC operation. This character shows that, the use of re-boiler steam to adjust the power generation may effectively improve the load tracking ability of the CFPP without much influence on the PCC operation.

Based on this insight, a collaborative control strategy is proposed for the integrated CFPP-PCC plant. The re-boiler steam flowrate is incorporated into the MPC of CFPP, which is manipulated for the CFPP load ramping and then gradually set to the required value for CO_2 capture. The PCC is thus operating as an energy storage device, which can shift the charging rate continually during the FFFPS load change, providing the plant with additional flexibility. It is found that the proposed collaborative strategy can effectively accelerate the load ramping speed of the CFPP, shorten the transition period and minimize the tracking error, especially for small range of load change. Meanwhile, by designing another MPC to rationally manipulate the lean solvent flowrate, only small operation performance degradation is viewed for the PCC system. The results convincingly demonstrate the advantages of the proposed collaborative control strategy and show potential function of PCC in improving the flexibility of the CFPP. The approach is not only limited to CFPP-PCC system, but can be easily applied to other FFFPSs such as the CCGT plant equipped with solvent-based PCC device.

The dynamic performance of different PCC control schemes is also assessed. The results show that when the re-boiler steam flowrate is used for CFPP load regulation for the short term, it is impossible for the PCC system to maintain the CO_2 capture level and re-boiler temperature if the lean solvent flowrate remains constant. The control scheme which keeps the L/G ratio constant is feasible in the CFPP load following scenario but fails in the case of CO_2 capture level change. The PI and MPC control schemes can provide better operating performance. Moreover, it is observed that the PCC system presents superior dynamic control performance when lean solvent flow is manipulated to control the capture level, whilst controlling the re-boiler temperature can result in better economic performance for the PCC system.

Acknowledgements

The authors would like to acknowledge the National Natural Science Foundation of China (NSFC) under Grants 51976030 and 51936003, Natural Science Foundation of Jiangsu Province for Outstanding Young Scholars under Grant BK20190063, the Royal Society - Sino British Fellowship Trust International Fellowship (REF: NIF\R1\181257), EU FP7 International Staff Research Exchange Scheme on power plant and carbon capture (Ref: PIRSES-GA-2013-612230) and the Fundamental Research Funds for the Central Universities for funding this work.

References

[1] IEA, Electricity information 2017, IEA Publications, Aug. 2017. https://euagenda.eu/publications/electricity-information-2017, Accessed on 22th Sep

2019.

[2] UNFCCC, Historic Paris Agreement on Climate Change, from http://newsroom.unfccc.int/unfccc-newsroom/finale-cop21/, Accessed on 22th Sep 2019.

[3] Global CCS Institute, The Global Status of CCS: 2018, GCCSI, Oct. 2018. https://www.globalccsinstitute.com/resources/global-status-report/, Accessed on 22th Sep 2019.

[4] M. B. Blarke. Towards an intermittency-friendly energy system: comparing electric boilers and heat pumps in distributed cogeneration. Applied Energy 2012; 91:349–65.

[5] National Energy Administration of China. The statistics of wind power integration in 2016. 2017. http://www.nea.gov.cn/2017-01/26/c_136014615.htm, Accessed on 22th Sep 2019.

[6] X. Wu, J. Shen, Y. Li, and K. Y. Lee. Steam power plant configuration, design and control. WIREs Energy Environ 2015; 4(6): 537-563.

[7] M. Bui, I. Gunawan, V. Verheyen, P. Feren, E. Meuleman and S. Adeloju. Dynamic modelling and optimisation of flexible operation in post-combustion CO_2 capture plants — A review. Computers and Chemical Engineering 2014; 61: 245-265.

[8] N. Mac Dowell and N. Shah. The multi-period optimisation of an amine-based CO_2 capture process integrated with a super-critical coal-fired power station for flexible operation. Computers and Chemical Engineering 2015; 74: 169-183.

[9] A. K. Olaleye, E. Oko, M. Wang, and G. Kelsall. Dynamic modelling and analysis of supercritical coal-fired power plant integrated with post-combustion CO_2 capture. Clean Coal Technology and Sustainable Development: Proceedings of the 8th International Symposium on Coal Combustion, pp. 359-363, Springer Science+ Business Media Singapore and Tsinghua University Press, Singapore, 2016.

[10] X. Wu, M. Wang, P. Liao, J. Shen, and Y. Li. Solvent-based post-combustion CO_2 capture for power plants: a critical review and perspective on dynamic modelling, system identification, process control and flexible operation. Applied Energy 2020; 257.

[11] C. Biliyok, A. Lawal, M. Wang, and F. Seibert. Dynamic modelling, validation and analysis of post-combustion chemical absorption CO_2 capture plant. International Journal of Greenhouse Gas Control 2012; 9: 428–445.

[12] N. A. Manaf, A. Cousins, P. Feron, and A. Abbas. Dynamic modelling. Identification and preliminary control analysis of an amine-based post-combustion CO_2 capture pilot plant. Journal of Cleaner Production 2016; 113: 635-653.

[13] J. Gáspár, A. Gladis, J. B. Jøgensen, K. Thomsen, N. Solms, and P. L. Fosbøl. Dynamic Operation and Simulation of Post-Combustion CO_2 Capture. The 8th Trondheim Conference on CO_2 Capture, Transport and Storage. Energy Procedia 2016; 86: 205–214.

[14] N. Enaasen, L. Zangrilli, A. Mangiaracina, T. Mejdell, H. M. Kvamsdal, and M. Hillestad. Validation of a Dynamic Model of the Brindisi Pilot Plant. 12th international conference on Greenhouse Gas Control Technologies (GHGT-12). Energy Procedia 2014; 63: 1040–1054.

[15] X. Wu, J. Shen, Y. Li, M. Wang, and A. Lawal. Nonlinear dynamic analysis and control design of a solvent-based post-combustion CO_2 capture process, Computers & Chemical Engineering 2018; 115: 397-406.

[16] E. Mechleri, A. Lawal, A. Ramos, J. Davison, and N. Mac Dowell. Process control strategies for flexible operation of post-combustion CO_2 capture plants. International Journal of Greenhouse Gas Control 2017; 57: 14-25.

[17] S. Posch and M. Haider. Dynamic modeling of CO_2 absorption from coal-fired power plants into an aqueous monoethanolamine solution. Chemical Engineering Research and Design 2013; 91: 977-987.

[18] Y. Lin, C. Chang, D. Wong, S. Jang, and J. Ou. Control Strategies for Flexible Operation of Power Plant with CO_2 Capture Plant. Proceedings of the 11th International Symposium on Process Systems Engineering, 2012, pp. 1366-1371.

[19] T. Nittaya, P. L. Douglas, E. Croiset, and L. A. Ricardez-Sandoval. Dynamic modelling and control of MEA absorption processes for CO_2 capture from power plants. Fuel 2014; 116: 672-691.

[20] X. Wu, J. Shen, Y. Li, M. Wang, and A. Lawal. Flexible operation of post-combustion solvent-based carbon capture for coal-fired power plants using multi-model predictive control: a simulation study. Fuel 2018; 220: 931-941.

[21] E. D. Mechleri, N. Mac Dowell, and N. F. Thornhill. Model predictive control of post-combustion CO_2 capture process integrate with a power plant. 12th International Symposium on Process Systems Engineering and 25th European Symposium on Computer Aided Process Engineering, Copenhagen, Denmark, May 31-June 4, 2015.

[22] M. T. Luu, N. A. Manaf, and A. Abbas. Dynamic modelling and control strategies for flexible operation of amine-based post-combustion CO_2 capture systems. International Journal of Greenhouse Gas Control 2015; 39: 377-389.

[23] B. Decardi-Nelson, S. Liu, and J. Liu. Improving Flexibility and Energy Efficiency of Post-Combustion CO_2 Capture Plants Using Economic Model Predictive Control. Processes 2018; 6: 135.

[24] S. Oh, S. Yun, and J. Kim. Process integration and design for maximizing energy efficiency of a coal-fired power plant integrated with amine-based CO2 capture process. Applied Energy 2018; 216: 311-322.

[25] IEAGHG, Evaluation of process control strategies for normal, flexible, and upset operation conditions of CO_2 post combustion capture processes. 2016/07, in, IEAGHG, September 2016.

[26] A. Lawal, M. Wang, P. Stephenson, and O. Obi. Demonstrating full-scale post-combustion CO_2 capture for coal-fired power plants through dynamic modelling and simulation. Fuel 2012; 101: 115-128.

[27] R. M. Montañés, S. Ó. GarÐarsdóttir, F. Normann, F. Johnsson, and L. O. Nord. Demonstrating load-change transient performance of a commercial-scale natural gas combined cycle power plant with post-combustion CO_2 capture. International Journal of Greenhouse Gas Control 2017; 63: 158-174.

[28] X. Wu, M. Wang, J. Shen, Y. Li, A. Lawal, and K. Y. Lee. Flexible operation of coal fired power plant integrated with post combustion CO_2 capture using model predictive control. International Journal of Greenhouse Gas Control 2019; 82: 138-151.

[29] X. Wu, M. Wang, J. Shen, Y. Li, A. Lawal, and K. Y. Lee. Reinforced coordinated control of coal-fired power plant retrofitted with solvent based CO_2 capture using model predictive controls. Applied Energy 2019; 238: 495-515.

[30] P. Liao, Y. Li, X. Wu, M. Wang, and E. Oko. Flexible operation of large-scale coal-fired power plant integrated with solvent-based post-combustion CO_2 capture based on neural network inverse control. International Journal of Greenhouse Gas Control 2020; 95: 1-15.

[31] J. Rodriguez, A. Andrade, A. Lawal, N. Samsatli, S. Calado, T. Lafitte, J. Fuentes, and C. Pantelides. An integrated framework for the dynamic modelling of solvent-based CO_2 capture processes. Energy Procedia, vol.63, pp. 1206-1217, 2014.

[32] A. Lawal, M. Wang, P. Stephenson, G. Koumpouras, and Yeung H. Dynamic modelling and analysis of post-combustion CO_2 chemical absorption process for coal-fired power plants. Fuel, vol. 89, pp. 2791-2801, 2010.

[33] X. Wu, J. Shen, M. Wang, and K. Y. Lee. Intelligent predictive control of large-scale solvent-based CO_2 capture plant using artificial neural network and particle swarm optimization. Energy 2020; 196: 1-14.

[34] D. Q. Mayne, J. B. Rawings, and C. V. Rao. Constrained model predictive control: Stability and optimality. Automatica 2000; 36: 789 – 814.

[35] S. J. Qin. An overview of subspace identification. Computers and Chemical Engineering 2006; 30: 1502–1513.